Naval Research Laboratory
Washington, DC 20375-5320

NRL/5540/MR—2021/6

Euclidean Representations of Quantum Information

TANNER CROWDER

Center for High Assurance Computer Divisions
Information Technology Division

October 5, 2021

REPORT DOCUMENTATION PAGE

Form Approved
OMB No. 0704-0188

1. REPORT DATE *(DD-MM-YYYY)*	**2. REPORT TYPE**	**3. DATES COVERED** *(From - To)*
05-10-2021	NRL Memorandum Report	10/01/2017 – 09/30/2021

4. TITLE AND SUBTITLE

Euclidean Representations of Quantum Information

5a. CONTRACT NUMBER

5b. GRANT NUMBER

5c. PROGRAM ELEMENT NUMBER

6. AUTHOR(S)

Tanner Crowder

5d. PROJECT NUMBER

5e. TASK NUMBER

5f. WORK UNIT NUMBER
1G28

7. PERFORMING ORGANIZATION NAME(S) AND ADDRESS(ES)

Naval Research Laboratory
4555 Overlook Avenue, SW
Washington, DC 20375-5320

8. PERFORMING ORGANIZATION REPORT NUMBER

NRL/5540/MR--2021/6

9. SPONSORING / MONITORING AGENCY NAME(S) AND ADDRESS(ES)

Office of Naval Research
One Liberty Center
875 N. Randolph Street, Suite 1425
Arlington, VA 22203-1995

10. SPONSOR / MONITOR'S ACRONYM(S)

ONR

11. SPONSOR / MONITOR'S REPORT NUMBER(S)

12. DISTRIBUTION / AVAILABILITY STATEMENT

DISTRIBUTION STATEMENT A: Approved for public release; distribution is unlimited.

13. SUPPLEMENTARY NOTES

14. ABSTRACT

The purpose of this document is to provide an overview of the work done under the basic research project Euclidean Representations of Quantum Information.

15. SUBJECT TERMS

16. SECURITY CLASSIFICATION OF:			**17. LIMITATION OF ABSTRACT**	**18. NUMBER OF PAGES**	**19a. NAME OF RESPONSIBLE PERSON**
					Tanner Crowder
a. REPORT	**b. ABSTRACT**	**c. THIS PAGE**	U	34	**19b. TELEPHONE NUMBER** *(include area code)*
U	U	U			(202) 404-8224

This page intentionally left blank.

CONTENTS

FIGURES

TABLES

This page intentionally left blank

EXECUTIVE SUMMARY

The purpose of this document is to provide an overview of the work done under the basic research project "Euclidean Representations of Quantum Information."

This page intentionally left blank

EUCLIDEAN REPRESENTATIONS OF QUANTUM INFORMATION

1. BACKGROUND

There is a mismatch between the standard Hilbert space formalism of quantum mechanics and the current communication problems in information technology. Consequently, basic problems like quantitatively measuring information flow through a quantum channel remain ambiguous. In addition, when performing standard measurement procedures on a quantum system, e.g., tomography, one does not produce an element of the Hilbert space, but instead a collection of expected values obtained by measuring observables. As an example, when measuring the polarization state of a photon using the stokes parametrization, one obtains a real three-vector, where each entry corresponds to the measurement of a fixed observable. The vector is called the Bloch representation of the quantum state, and each qubit can be uniquely described by such a vector. The elegance of the Bloch representation lies within its ability use basic Euclidean notions, allowing for easier mathematical manipulations and manageable calculations of information theoretic quantities. However, the mathematical foundation is lacking for a Bloch representation for quantum systems larger than a qubit. In order to fully utilize the power of quantum information and address the concerns of information technology, our objective was to develop a Euclidean representation for higher-dimensional systems and use it as a guide to the experimental realization of new quantum technologies.

2. QUANTUM INFORMATION THEORY

Associated to any isolated physical system is a complex vector space with inner product, we call this the *state space*. The system is completely described by a unit vector in the state space called a *state vector*. We denote the state vectors as $|\psi\rangle$ and the inner product is written $\langle\psi|\phi\rangle$, where $\langle\psi|$ is taken to be $|\psi\rangle^\dagger$. When the state is not completely known, we use *mixed states* to describe the system; these are ensembles of pure states, $\{p_i, |\psi_i\rangle\}$, which is read as with probability p_i the system is in the state $|\psi_i\rangle$. Let $\mathcal{H}^2$ denote a two dimensional Hilbert space with the specified inner product $\langle\,\cdot|\cdot\rangle$. A unit vector in $\mathcal{H}^2$ can represent a two level quantum system which we call a qubit, or, the most basic form of quantum information.

In order to use a quantum system to store, transmit, or process information, we must be able to account for it's evolution. The evolution of any closed quantum system is described by a unitary operator, i.e., given a state $|\psi\rangle$ there is a unitary operator U such that $|\psi\rangle$ evolves to $U|\psi\rangle$. This evolution is theoretically reversible; however, often a quantum system will strongly couple to the environment, decohere, and the evolution is no longer unitary. There are two cases to consider for how the state of the system couples to the environment. Let the state of the system be ρ_s and the state of the environment be ρ_e. In the first case, the state of the system and the environment are in a pure tensor, i.e. the composite system is in the state $\rho_s \otimes \rho_e$. This coupling leads to *completely positive* dynamics. Most of the standard language of quantum information theory was written under the assumption of completely positivity. However, there are non-trivial instances when the system and environment do not couple in a pure tensor product, but instead become entangled. These dynamics lead to a highly non-trivial structure which were studied in both the previous 6.1 Base Program Project "Beyond the standard theory of quantum information," and in this project under the publications [1–3]; we will discuss

Manuscript approved September 27, 2021.

these dynamics further in subsequent sections of this report. For a majority of this report, we will assume complete positivity unless otherwise explicitly noted.

There are many ways to store, represent, process, and send quantum information. For example, we can use a quantum state to represent a classical bit of information and define the basic communication problem as follows. Alice and Bob choose an orthonormal basis for this state space

- The state $|\psi\rangle$ represents '0'
- The state $|\phi\rangle$ represents '1'
- $\langle\psi|\psi\rangle = 1$, $\langle\phi|\phi\rangle = 1$, and $\langle\psi|\phi\rangle = 0$

With this identification, we have implicitly defined a classical channel:

- Alice sends a qubit $|*\rangle$ representing '0' or '1' to Bob.
- As the qubit $|*\rangle$ travels, it interacts with the environment, changing to $\varphi(|*\rangle)$
- Bob receives and measures the qubit, obtaining a '0' or '1'.

These channels are binary channels and have two inputs and two outputs ("1" and "0"). The transmission of information can be modeled by the noise matrix

$$u = \begin{pmatrix} x & \overline{x} \\ y & \overline{y} \end{pmatrix}, \tag{1}$$

where x is the probability of receiving a 0 when a 0 is sent, $\overline{x} = 1 - x$ is the probability of receiving a 1 when a 0 is sent, y is the probability of receiving a 0 when a 1 is sent and $\overline{y} = 1 - y$ is the probability of receiving a 1 when a 1 is sent. The noise matrix can also be represented as (x, y), which is a point on the unit square $[0, 1]^2$. The binary symmetric channels occur when $y = 1 - x$, or as a point on the anti-diagonal of $[0, 1]^2$. The *classical capacity* of this induced channel is the amount of classical information that can be transmitted through it. We can calculate the capacity of a qubit channel (with a fixed basis) as

$$C(x, y) = \log_2 \left(2^{\frac{\bar{x}H(y) - \bar{y}H(x)}{x - y}} + 2^{\frac{yH(x) - xH(y)}{x - y}} \right), \tag{2}$$

where $H(x) = -x \log_2(x) - (1 - x) \log_2(1 - x)$ is the Shannon entropy [4]. From previous base program work on "A new mathematical representation of quantum information," we know that each choice of basis induces its own classical channel, with its own capacity; the *scope* is the range of capacities as we vary over every basis in the state space [5]. While eqn. 2 provides a closed for solution for calculating capacity, the current mathematical language for quantum mechanics makes it cumbersome to employ. For example, assume that a channel behaves as follows: with probability q the unitary operation

$$\sigma_3 = \begin{pmatrix} 0 & -i \\ i & 0 \end{pmatrix}$$

is applied, and with probability $1-q$, the identity operator is applied. This channel is a natural analog to the classical bit flipping channel, and is one of the easiest non-trivial channels to describe. Lets consider the orthonormal states $|\psi\rangle = a|0\rangle + b|1\rangle$ and $|\phi\rangle = c|0\rangle + d|1\rangle$. Then the probabilities for the capacity calculation are as follows:

$$x = (1-q)|a|^4 + (2q+2)|a|^2|b|^2 + (1-q)b^4 \quad (3)$$

$$y = 1 - ((1-q)|c|^4 + (2q+2)|c|^2|d|^2 + (1-q)|d|^4). \quad (4)$$

To calculate the scope then, and to maximize the bandwidth by choosing the optimal representation, we must be able to systematically calculate the range of capacities as we vary over every basis of the state space.

When systems become larger, a classical channel can have m inputs and n outputs. The noise is modeled by an $m \times n$ stochastic matrix. Generally, we restrict ourselves to the case where $m = n$; however, as the system size grows so does the complexity of the capacity calculations. For all but the binary channel, there is no closed for solution to the capacity for an (m, m) channel. Additionally, one of the chief functions of quantum information is to utilize and distribute entanglement. It is therefore necessary to consider the problem of distributing this quantum information, and quantifying the resources necessary to do it. In the following, we will discuss how the *Bloch representations* ease the calculations of informatic quantities for the qubit, and the structure of its extension to n-qubit systems, which we call *the Euclidean representation of quantum information*. We will present an overview of the results derived from this project, with citations for a complete description, as well as some of the more recent, yet to be published work that is still in preparation being done in conjunction with other ongoing projects.

3. EUCLIDEAN REPRESENTATIONS

Quantum mechanics is a theoretical framework that is used to describe the behavior of a physical system. The postulates of quantum mechanics describe the mathematical structure necessary to describe quantum systems and their evolution [6]. However, the postulates do not give a procedure for describing the polarization state of a photon for example, only that there exists some unit vector in a Hilbert space that describes that state. A quantum state can be defined in a multitude of ways, either through the state vector approach, as mentioned, or the density operator approach.

Definition 1 The *density operator* for an n-qubit system is a trace one, positive semi-definite, $2^n \times 2^n$ Hermitian matrix.

Because the space of Hermitian matrices form a vector space, we can expand them in terms of a basis. Consider the spin operators

$$\sigma_2 = \begin{pmatrix} 0 & 1 \\ 1 & 0 \end{pmatrix}, \ \sigma_3 = \begin{pmatrix} 0 & -i \\ i & 0 \end{pmatrix}, \text{ and } \ \sigma_4 = \begin{pmatrix} 1 & 0 \\ 0 & 1 \end{pmatrix}. \quad (5)$$

These matrices are orthogonal in the Hilbert-Schmidt inner product and together with the two dimensional identity, $I_2 = \sigma_1$, they form a basis for the 2×2 Hermitian matrices, and thus can be used to represent a qubit.

Definition 2 The state of a qubit can be written as

$$\rho = \frac{I + r \cdot \sigma}{2},$$

where $r \in \mathbb{R}^3$. The vector r is called the *Bloch vector*.

One can readily show that the collection of Bloch vectors for the qubit is equal to the unit ball in $\mathbb{R}^3$. But moreover, the elements of the Bloch vector correspond to the expectation values of actual physical measurements. For the polarization state of the photon, they correspond to the expectation values of measuring in the horizontal/vertical, diagonal/anti-diagonal, and right/left circular bases.

We've described the general framework for quantum evolution, but here we will be precise with respect to n-qubits:

Definition 3 *An n-qubit quantum channel is a (completely) positive, trace-preserving, linear map.*

We put 'completely' as a parenthetical because it should not be strictly enforced as a definition, but will be assumed for the most part. Since these maps are linear, they are completely determined on a basis. Therefore, in a similar way to the construction of the Bloch vector, we can construct the Bloch representation of a qubit channel.

Definition 4 A qubit channel, ε induces a affine map φ on the Bloch vector as follows,

$$\varepsilon\left(\frac{I + r \cdot \sigma}{2}\right) = \frac{I + \varphi(r) \cdot \sigma}{2}; \tag{6}$$

φ is called the *Bloch representation* of the channel and has the form $\varphi(r) = Mr + b$. When φ is linear, the channel is called unital.

We will focus on unital channels because they form a conservative model of noise [7]. But additionally, we describe some work we have done on non-unital channels as well.

Using the Bloch representation, we can simplify the calculation of informatic quantities. For example, recall the classical probabilities defined by eqn. 3. Instead of trying to maximize the capacity using them, we can calculate the range of capacities using its Bloch representation. In this case, the channel is unital and has the following Bloch matrix

$$M = \begin{pmatrix} 1-2q & 0 & 0 \\ 0 & 1 & 0 \\ 0 & 0 & 1-2q \end{pmatrix} \tag{7}$$

Using results from [5], the scope of this channel is $s(M) = [1 - H(q), 1]$ when $q < 1/2$, and $s(M) = [0, 1]$ otherwise. More generally, it was shown in [5] that if f is a unital channel, its scope can always be calculated

from the eigenvalues of its symmetric part $(f + f^t)/2$. If the eigenvalues are ordered as $\lambda_1 \leq \lambda_2 \leq \lambda_3$, then the scope of f is

$$s(f) = \left[\frac{1 + \text{sgn}(\lambda_1\lambda_3)}{2}\left(1 - H\left(\frac{1 + \min|\lambda_i|}{2}\right)\right), 1 - H\left(\frac{1 + \max|\lambda_i|}{2}\right)\right]. \tag{8}$$

This is just one application of the Bloch representation. Because the chief quantum resource, entanglement, happens in systems larger than a qubit, it is reasonable to wonder if such a representation exists for systems of larger dimension. Much like the case for the qubit, we will expand the n-qubit density matrices in terms of a basis of measurement operators. Each choice of basis induces a new Euclidean representation. Here we will discuss the most popular one:

Definition 5 Define $\left\{\sigma_{j_1} \otimes \cdots \otimes \sigma_{j_n} | j_i \in \{1, 2, 3, 4\}\right\}$ to be the set of *n-qubit spin operators*. Order them with the dictionary order and label the i^{th} matrix in the order λ_i.

Since the n-dimensional spin operators are the n-fold tensor products of orthogonal and linearly independent matrices, they as well form an orthogonal and linearly independent set. Moreover, if $A, B \in M_k(\mathbb{C})$, then $(A \otimes B)^\dagger = A^\dagger \otimes B^\dagger$. Thus the n-dimensional spin operators are contained in the $2^n \times 2^n$ Hermitian matrices; since there are 4^n of them, they must form a basis. Similar to the qubit case, vectorize the last $4^n - 1$ as $\lambda^n = [\lambda_2^n\ \lambda_3^n\ \cdots\ \lambda_{4^n}^n]^t$. Given $A, B \in M_k(\mathbb{C})$, $\text{tr}(A \otimes B) = \text{tr}(A)\text{tr}(B)$, thus each entry of λ is a traceless matrix. We can therefore write each density matrix as

$$\rho = \frac{I + cr \cdot \lambda}{2^n},$$

where $c = \sqrt{2^n - 1}$.

Definition 6 The vector r in the above expansion of a density matrix is called the *Bloch vector*.

Note, the constant c ensures that the Bloch vector corresponding to pure states has norm 1. Similar to the qubit, a quantum channel ε induces an affine map on the Euclidean representation of a state:

$$\varepsilon\left(\frac{I + cr \cdot \lambda}{2^n}\right) = \frac{I + c\varphi(r) \cdot \lambda}{2^n}.$$

These maps are of critical importance in understanding the informatic properties of higher-dimensional systems.

Definition 7 Let $\rho = 1/2^n(I + cr \cdot \lambda)$ be a density matrix and let ε be a quantum channel defined as

$$\varepsilon(\rho) = \frac{I + c\varphi(r) \cdot \lambda}{2^n},$$

where $\varphi(r) = fr + b$. Then φ is the *Bloch representation* of the channel ε.

These higher dimensional Euclidean representations share similarities those for the qubit. For example, there is a convex-linear bijection that identifies density operators and channels to their Euclidean representations [8]. For the Euclidean representation, the states and channels arise as expectation values of measurements, and informatic quantities can be calculated from them; however, we must differentiate them from the single qubit because, while similar to the qubit, the differences must be treated with care. For example, the state space for the qubit is the entire unit ball, usually referred to as the Bloch sphere. Does such a ball exist in higher dimensions? Let r be the vector where all the entries corresponding to the non-diagonal spin operators are 0 and the entries corresponding to the diagonal spin operators are $-1/c$. Since only σ_1 and σ_4 are diagonal, there are $2^n - 1$ diagonal spin operators in λ; so the Bloch vector described above has norm $2^{n-1}/c^2 = 1$. Since the $(1,1)$ entry of σ_1 and σ_4 is 1, the n-fold tensor product of a combination of them will have a 1 in the $(1,1)$ position. Therefore in arbitrary dimensions the $(1,1)$ position of the density matrix we described is $\frac{1}{2^n}(1 - \frac{2^n-1}{c})$. Since $2^n - 1 > \sqrt{2^n - 1}$, we know that $\frac{2^n-1}{c} > 1$ implying $0 > 1 - \frac{2^n-1}{c}$. Since the matrix is diagonal and has a non-positive entry, it is not a valid density operator. Thus the vector has norm 1, but is not a Bloch vector. When $n = 2$ the resulting density matrix is

$$\begin{pmatrix} -1/2 & 0 & 0 & 0 \\ 0 & 1/2 & 0 & 0 \\ 0 & 0 & 1/2 & 0 \\ 0 & 0 & 0 & 1/2 \end{pmatrix} \tag{9}$$

which is not positive-semidefinite. Therefore, the state space is not a ball using these spin-operators. However, as we mentioned, we could choose many orthonormal bases to expand the quantum system, maybe there are others. We have the following result, proven in [9]:

Theorem 8 *For the set of quantum states Ω^n, the following are equivalent:*

- *(i) There is a convex linear bijection from the Ω^n to a ball in R^m.*
- *(ii) The dimension of the underlying state space is $n = 2$.*
- *(iii) There is a convex linear involution $* : \Omega^n \to \Omega^n$ whose only fixed point is I^n.*

As a surprising corollary to that statement, we can show that if r is the Euclidean representation of a pure state, it's antipode is not the Euclidean representation of any state. While the last theorem implies that the algebraic and geometric structure of the Euclidean representations of quantum information is highly non-trivial, it does lend itself useful [10].

We mostly discuss Euclidean representations in terms of the basis of n-dimensional spin operators. However, any basis of mutually orthogonal observables would be sufficient to construct a Euclidean representation. Using the chi matrix representation would build a Euclidean representation of the evolution dynamics. Additionally we provided necessary extremal conditions for the convex set of channels using the chi matrix representation. For the single qubit unital channels, the extreme points are exactly those induced by unitary conjugation, i.e. all evolution can be written as the non-deterministic choice between unitary evolutions. While the class of (completely positive) trace preserving linear maps is a closed and bounded set, and hence compact [8], for larger dimensions the extreme points are more difficult to describe [11]. In [11], there is fantastic characterization of extremality conditions. The hope for this effort though would be to provide conditions which answer questions about whether or not the extreme points were path connected, as in the case of the single qubit, providing a continuous method to map between quantum operations.

3.1 Teleportation

Using the Euclidean representations of quantum information, we can characterize the set of n-qubit channels that are diagonal in the Bloch representation. These channels are extremely important for calculating the scope of a single qubit channel, and are proving useful in larger dimensions as well. The characterization is as follows:

Theorem 9 *Let $N = 2^n$ and $\Phi_D : H_N \to H_N$ be a operator given by*

$$\Phi_D\left(\frac{I + \vec{r}\cdot\vec{\lambda}}{N}\right) = \frac{I + D\vec{r}\cdot\vec{\lambda}}{N},$$

where

$$D = \begin{pmatrix} d_2 & 0 & 0 \\ 0 & \ddots & 0 \\ 0 & 0 & d_N \end{pmatrix} \text{ and let } \vec{d} = \begin{pmatrix} 1 \\ d_2 \\ \vdots \\ d_N \end{pmatrix}.$$

Φ_D is completely positive, and hence a unital operation, if and only if $H^{\otimes n}\vec{d}$ has all non-negative entries.

Alternatively, we can look at the set of channels induced by conjugation by spin-operators, $\varepsilon_i(\rho) := \lambda_i \rho \lambda_i$. These higher-dimensional spin channels are diagonal and invertible, like their single qubit counterparts. Also though, they form the set of extreme points for the convex set of diagonal channels; i.e., any diagonal channel can be written as a convex sum of the higher dimensional spin channels. In conjunction with the NISE project "Noise Characterization of Quantum Teleportation with Imperfectly Prepared States," we completely characterized the Euclidean representation of 2-qubit teleportation channels using non-pure state entanglement. As discussed in [12], we showed that the set of noisy 2-qubit teleportation channels is equal to the set of of 2-qubit diagonal channels. We were able to leverage the work done in this project to provide lower bounds for the amount information that could be transferred with these systems. While exotic sounding, teleportation is the phenomena that underpins entanglement swapping and repeater technologies that will most likely be necessary to realize quantum networking protocols. As we move toward implementing networking protocols that may implement these technologies, we will need the ability to readily assess the components for use. The complete noise model given by teleportation channels, and the ability to compute lower bounds for information transfer, will assist in that effort.

3.2 Quantum Information in Relativity

In conjunction with the base program project "Quantum information in gravity," we extended results from the project "Beyond the standard theory of quantum information" to relativistic settings. We show that using an imperfectly prepared state in relativistic settings, the evolution of a massive spin-1/2 particle violates many standard assumptions made in quantum information theory, including complete positivity. Unlike other recent endeavors in relativistic quantum information, we are able to quantify and maximize how much information can be transferred through such a quantum process by calculating its scope. We show that, surprisingly, relativistic noise can increase the amount of information that can be transferred, and in fact,

even if the initial state is arbitrarily close to the completely mixed state, information can still be transferred perfectly. Additionally, we explore the relativistic effects of velocity and gravity on quantum information processing, and we briefly discuss how quantum computation is affected by general relativity. In particular, we show that the large Wigner rotation caused by a black hole as described in the Schwarzschild metric can greatly increase the informatic content of certain imperfectly prepared qubits. As we move from terrestrial based quantum information systems, to spaced based systems, we must consider the effects of relatively, much like we account for its effects in GPS navigation.

We will forgo the standard introduction to quantum mechnaics in a relativistic field and focus on how quantum information is altered by these effects. For a complete discussion on this background, see [1, 2] and the sources therein. While noise is extremely common in quantum information processing, generally, quantum information protocols implicitly assume idealized conditions for state generation and measurement. However, generating on demand qubits for information processing is difficult. Here, we consider an improperly prepared massive spin-1/2 state with spin-momentum entanglement. To analyze this effect, we took a somewhat toy model and assume that we have a black box emitting the state

$$|\Psi\rangle = r|p, 0\rangle + s|q, 1\rangle, \tag{10}$$

with $|r|^2 > |s|^2$. We assume that momentum and spin are described by a fixed axis with respect to frame of reference, which all parties have knowledge of. Upon tracing out the momentum, i.e., just measuring the spin of the system, the reduced state is

$$\rho = \mathrm{tr}_p(|\Psi\rangle\langle\Psi|) = \begin{pmatrix} |r|^2 & 0 \\ 0 & |s|^2 \end{pmatrix}. \tag{11}$$

This state looks like an imperfectly prepared spin state, and it may be determined that for information processing purposes it is an adequate approximation of the pure state.

We completely characterized evolution of an arbitrary state using staters like these. It is important to note that these arbitrary states had to be accounted for with care. In this example, we cannot assume access to the entire state space since we are implicitly assuming that the initial states have spin momentum entanglement. To represent an arbitrary spin state $|\phi\rangle\langle\phi|$, we preformed a local unitary operation $I \otimes V|\Psi\rangle$, where V was chosen in such a way that $|V\rangle|0\rangle = |\psi\rangle$. In [1, 2], we showed that, although many such unitary operations will map $|0\rangle$ to ϕ, this was a well defined operation. The reduced state of the system is then

$$|r|^2|\phi\rangle\langle\phi| + |s|^2|\phi^\perp\rangle\langle\phi^\perp|. \tag{12}$$

where $|\phi^\perp\rangle = V|1\rangle$. Then, on a state of the form

$$\omega = |r|^2|\phi\rangle\langle\phi| + |s|^2|\phi^\perp\rangle\langle\phi^\perp|, \tag{13}$$

we define the map

$$\varepsilon(\omega) = \mathrm{tr}_p(\hat{U}(I \otimes V)|\Psi\rangle\langle\Psi|(I \otimes V)^\dagger\hat{U}^\dagger), \tag{14}$$

which describes the local dynamics under a global Lorentz transformation. Since $\mathrm{tr}\,(\omega) \neq \mathrm{tr}\,(\omega^2)$, there is no way to generate a pure state with the black box [6]. It would then be meaningless to ask what $\varepsilon(|\phi\rangle\langle\phi|)$ is. However, we can form all convex combinations of states like ω, and ask how ε operates on them; that convex hull is the *state space*. We showed that this map is well defined on our state space.

To analyze the informatic properties of this map we considered its Bloch representation. The Bloch matrix for ε is

$$f = \frac{1}{|r|^2 - |s|^2} \begin{pmatrix} |r|^2 \cos\Omega_p - |s|^2 \cos\Omega_q & 0 & -|r|^2 \sin\Omega_p + |s|^2 \sin\Omega_q \\ 0 & |r|^2 - |s|^2 & 0 \\ |r|^2 \sin\Omega_p - |s|^2 \sin\Omega_q & 0 & |r|^2 \cos\Omega_p - |s|^2 \cos\Omega_q \end{pmatrix}. \tag{15}$$

Although f has the appearance of a standard Bloch matrix, f is an expansive map, so it does not map the unit ball to itself, and thus it does not always map states to states. However, it does map states from the reduced state space to itself. Since f is expansive it will not increase the *von Neumann entropy*

$$S(\rho) = -\lambda_+ \log_2(\lambda_+) - \lambda_- \log_2(\lambda_-) \tag{16}$$

of a state. We have plotted the von Neumann entropy as a function of the Wigner angle in fig. 1 where we have fixed the values of $r = \sqrt{9/10}$ and $s = \sqrt{1/10}$. Contrary to most standard dynamics, this map decreases

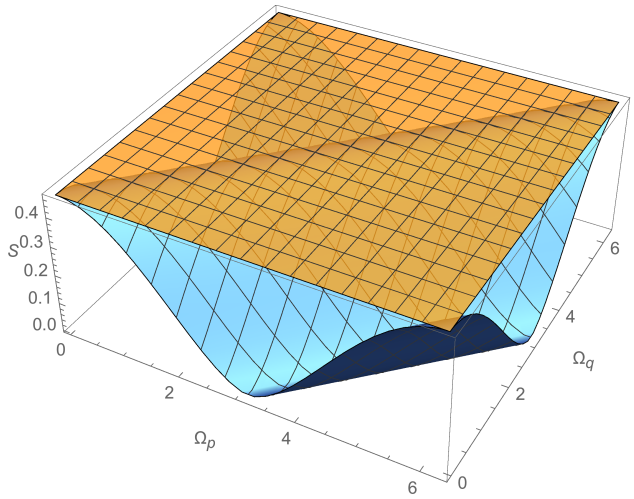

Fig. 1—Plot of the entropy pre- and post-evolution for the state in eqn. (11) with $r = \sqrt{9/10}$ and $s = \sqrt{1/10}$. The plane gives reference to the entropy pre-evolution, whereas the entropy post-evolution varies with Ω_p and Ω_q.

the von Neumann entropy almost everywhere with respect to the Lebesgue measure.

As the states are not becoming more mixed, and thus becoming more pure, it is reasonable to ask how this affects information transfer. Generally, when classical information is sent through a quantum process, states are prepared and measured in the same basis, and they are not measured with an idealized basis. For this reason, in general, a positive information flow using an ideal measurement procedure does not correspond

to positive information flow using a fixed basis [13, 14]. To illustrate how this process affects information transfer, we have plotted the capacity in terms of the $\pm z$ and $\pm y$ communication bases in fig. 2, where $\{x, y, z\}$ is taken to be the standard basis in $\mathbb{R}^3$. It should be understood that when we speak about a communication

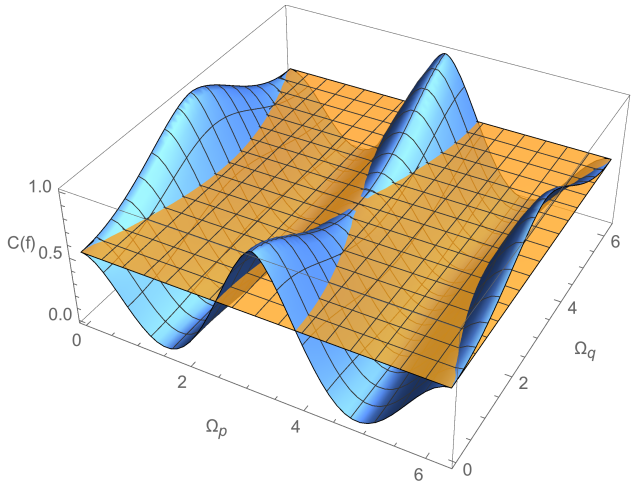

Fig. 2—The channel capacity when transmitting in the $\{\pm z\}$ basis (which varies over Ω_p and Ω_q) and the $\{\pm y\}$ basis (constant plane).

basis $\{\pm u\}$ we are preparing in the 0's and 1's as $\pm u \cdot (|r|^2 - |s|^2)$ and measuring with respect to the $\pm u$ basis. These calculations tell us that if the relativistic effects are large enough, the naive choice of basis is not the optimal one to transmit information. In addition, one choice of basis could lead to a channel with 0 capacity, while information could still be transferred with a different choice of basis. To study a specific example, let us take $r = \sqrt{9/10}$ and $s = \sqrt{1/10}$. Then if

$$|9/10\cos(\Omega_p) - 1/10\cos(\Omega_q)| \geq 8/10, \tag{17}$$

the optimal bases to transmit information are $\{x, -x\}$ and $\{z, -z\}$, because the $\{x, x\}$ and $\{z, -z\}$ bases correspond to the eigenvalues of largest magnitude for $1/2(f + f^t)$. Consequently, the process has a higher capacity than if one used the $\{y, -y\}$ basis, which is unaffected by relativistic noise. This fact goes against our natural intuition since $fy = y$, and thus $(8/10)y$ would not suffer the effects of the channel's noise. For a more extreme example, the initial state could be made arbitrarily close to the completely mixed state and information could be transferred perfectly.

We would also like to note that his process is not completely positive. For an arbitrary choice of r and s, (when $\Omega_p - \Omega_q \neq n\pi$) there will always be an eigenvalue of C that is negative, but so that the calculations

do not get out of hand, let's continue with $r = \sqrt{9/10}$ and $s = \sqrt{1/10}$. In this case, the Choi matrix is

$$\frac{1}{8}\begin{pmatrix} 9\cos^2\frac{\Omega_p}{2} - \cos^2\frac{\Omega_q}{2} & \frac{1}{2}(\sin\Omega_q - 9\sin\Omega_p) & \frac{1}{2}(9\sin\Omega_p - \sin\Omega_q) & 9\cos^2\frac{\Omega_p}{2} - \cos^2\frac{\Omega_q}{2} \\ \frac{1}{2}(\sin\Omega_q - 9\sin\Omega_p) & 9\sin^2\frac{\Omega_p}{2} - \sin^2\frac{\Omega_q}{2} & \sin^2\frac{\Omega_q}{2} - 9\sin^2\frac{\Omega_p}{2} & \frac{1}{2}(\sin\Omega_q - 9\sin\Omega_p) \\ \frac{1}{2}(9\sin\Omega_p - \sin\Omega_q) & \sin^2\frac{\Omega_q}{2} - 9\sin^2\frac{\Omega_p}{2} & 9\sin^2\frac{\Omega_p}{2} - \sin^2\frac{\Omega_q}{2} & \frac{1}{2}(9\sin\Omega_p - \sin\Omega_q) \\ 9\cos^2\frac{\Omega_p}{2} - \cos^2\frac{\Omega_q}{2} & \frac{1}{2}(\sin\Omega_q - 9\sin\Omega_p) & \frac{1}{2}(9\sin\Omega_p - \sin\Omega_q & 9\cos^2\frac{\Omega_p}{2} - \cos^2\frac{\Omega_q}{2} \end{pmatrix}. \tag{18}$$

Then ε is completely positive if and only if C is positive semi-definite [15]. However, the eigenvalues of C are 0, 0, and

$$1 \pm \frac{\sqrt{9\sin^2(\Omega_p/2 - \Omega_q/2) + 1}}{4}. \tag{19}$$

Since

$$1 - \frac{\sqrt{9\sin^2(\Omega_p/2 - \Omega_q/2) + 16}}{4} \in [-1/4, 0], \tag{20}$$

this process cannot be completely positive unless $\Omega_p - \Omega_q = 2n\pi$, in which case f is just a rotation of the Bloch sphere. Fig. 3 plots the negative eigenvalue of Choi's matrix as we range over Ω_p and Ω_q. It is well known that if the system and environment are in a pure product state, then the dynamics are completely positive; however, the converse is not necessarily true. Here the process is almost never completely positive, and there is an added degree of subtlety: instead of system-environment entanglement, the entanglement occurs across internal degrees of freedom.

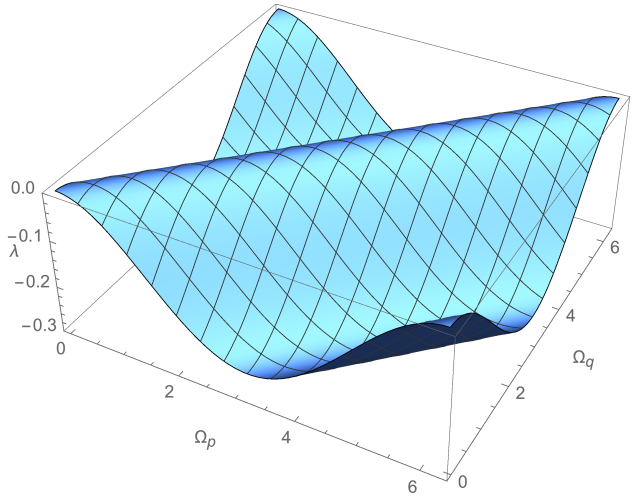

Fig. 3—The negative eigenvalue of C plotted with respect to Ω_p and Ω_q.

In summary, using fairly basic assumptions, we showed that relativistic quantum processes violate many standard assumptions made in quantum informatics by only assuming an imperfectly prepared state. As illustrated in fig. 3, the process is only completely positive on a set of measure zero. In addition, these processes are not exotic: preparing the state $|\Psi\rangle = r|p, 0\rangle + s|q, 1\rangle$ in the presence of a gravitational field would produce non-trivial Wigner rotations. Therefore (off that set of measure zero) the simple act of preparing and measuring the spin of such a state on Earth or on an orbiting satellite is not a completely positive process; albeit, this effect would be small and difficult to measure. We note that while these effects are small when only one particle is considered, they can accumulate during large quantum computations as we discuss in Section 3.3. The information in this section briefly discusses the work published in [1, 2] and can be referenced for a complete description of the technical details.

Finally, there have been discussions about the reduced density matrix in relativity, the appropriate measurement observables related to relativistic spin-1/2 particles [16–20], and whether or not the linear application of Wigner rotations creates a paradox. In [2], we address the issue of the amount to ascribe to a reduced density matrix, and in [3] we show that there is no paradox created by the linear application of Wigner rotations.

3.3 Quantum Computation

As apart of our work to characterize the Euclidean representations of relativistic noise, we thoroughly studied the effect of gravity on quantum computing systems. In this effort, we were able to improve the model given in [21] to provide an error correction technique similar to those provided by decoherence free subspaces. In [21], the noisy gravitation operator was represented as an approximation of a series expansion

$$I + \frac{i\Omega}{2} \sum_{j=1}^{n} \Delta_j + O(\Omega^2), \tag{21}$$

where

$$\Delta_j = \underbrace{I_2 \otimes \cdots \otimes I_2}_{j-1} \otimes \sigma_j \otimes \underbrace{I_2 \otimes \cdots \otimes I_2}_{n-j}, \tag{22}$$

Ω is the Wigner angle, and σ_j has a potentially different direction for each qubit. We however were able to supply an explicit formula for the Wigner rotation applied the an n-qubit system as

$$D = e^{i\Omega \sum_j \Delta_j / 2}. \tag{23}$$

Additionally, in [21], they assumed that the direction of the gravitational field was equal across the entire system. We did not make that assumption. Instead, we made a less restrictive assumption that the direction could vary from qubit to qubit, but that the direction stayed constant throughout the computation.

Using this new characterization of the gravity operator, we were able to show not only how gravity affected each qubit, but also how to structure a computation so that it is blind to gravity. We will omit the full details and direct the reader to [22], but will briefly discuss its impact. Unlike active error correcting codes, this technique employs a more passive structure to correct for the errors caused by gravity. While

there exist active error correcting codes and mechanical means to mitigate some noise sources, it is unknown how either apply to the decoherence induced by a gravitational field. Moreover, in this work we showed that while small, gravitational noise affects even the most basic computational steps; one such example is a basic single qubit operation which is an element in most basic quantum programming constructs. By choosing a clever embedding into a slightly larger system, we've shown that we can compute on a large number of those qubits, impervious to the deleterious effects of gravity. Additionally, as the number of qubits grow, the percentage that are accessible under this embedding does as well. For 100 qubits it is 96%, for 1000, it is 99.4%, and for 1,000,000 it is 99.9989%. In this vein, there are multiple subspaces that can be used in this way. As an example, for a 100-qubit system, there are seven complete 96-qubit subsystems that are unaffected by gravitational noise. Lastly, we would like to note that while this method was studied in the context of gravity and general relativity, we believe the it has much broader appeal. Any noise source that emits a form like eqn. 23, would have a similar analysis and could be handled likewise.

3.4 Non-unital Dynamics

We have thus far focused on multi-qubit channels and unital single qubit channels. These are the most natural quantum information processes. For a unital single qubit channel, it can always be written as a non-deterministic choice between unitary operations. However, the dynamics of amplitude damping are non-untial [6]. As pointed out in [6], these dynamics can arise from the spontaneous emission of a photon from an atom, or scattering within a single mode fiber. The first can been seen as applicable to certain quantum memory technologies, while the latter may be applicable to long range quantum networking and communications. However, these channels can be difficult to analyze from an information theoretic perspective. For example, let us consider the most general non-unital qubit channel $f(r) = Mr + x$. Define

$$\begin{aligned} a &:= \frac{1 + \langle r, f(r)\rangle}{2} = \frac{1}{2}(1 + \langle r, Mr\rangle + \langle r, b\rangle) \\ b &:= \frac{1 + \langle r, f(-r)\rangle}{2} = \frac{1}{2}(1 - \langle r, Mr\rangle + \langle r, b\rangle); \end{aligned} \tag{24}$$

that is, $a = P(0|0)$ is the probability that a 0 is measured when a 0 is sent, and $b = P(0|1)$ is the probability that a 0 is measured when a 1 is sent. The classical channel generated by f is denoted $x_f(r) = (a, b)$ and is an occupant of the unit square. However, it is not binary symmetric, and therefore we have to use the full capacity equation to quantify the effect of environmental noise. In addition, these channels have counterintuitive properties. From [23],

Theorem 10 *For any qubit channel $f(r) = Mr + x$ and any qubit $r \in \partial B^3$, we have $C(x_M(r)) \leq C(x_f(r))$. In fact, the scope of M and f are related by $M^- \leq f^- \leq M^+ \leq f^+$, where $M^\pm$ and $f^\pm$ are the upper and lower scope values of M and f.*

In other words, this theorem shows that, surprisingly, the non-unital part of a channel is a non-decreasing component of capacity. It is therefore difficult to answer, or predict, the behavior of these channels. For example, within the unital channels, the subset that has constant scope, i.e., no improvement can be made for adaptive quantum processing, has measure zero [5, 8, 13, 14, 23]. Is the same true for non-untial channels? Is the same true for amplitude dampening channels? Here we will discuss the progress made on these problems. The full solution is still a problem of interest.

We will denote the scope of the channel f as $s(f)$. We will frequently abuse the symbols f, a, and b to represent the quantities described above, as well as dynamical variables. We provided tools to estimate the capacity of certain classes of non-unital channels, and provided necessary conditions for when these channels' capacity is unchanged by a variation in the communication basis. Answering questions like these about non-unital quantum channels will help us address their informatic utility.

Lemma 11 *If f is a channel, and $R \in SO(3)$, then $s(R \circ f \circ R^t) = s(f)$.*

Proof. The set of classical channels generated by f are $\{(\langle r, fr\rangle, \langle r, f(-r)\rangle) : r \in \partial\mathbb{B}\}$. Rewriting $\langle r, R \circ f \circ R^t r\rangle = \langle R^t r, f(R^t r)\rangle$, the set of classical channels generated by $R \circ f \circ R^t$ is

$$\left\{(\langle r, fr\rangle, \langle r, f(-r)\rangle) : r \in R^t\partial\mathbb{B}\right\}.$$

Since $R^t\partial\mathbb{B} = \partial\mathbb{B}$, these two sets are equal, and therefore $s(f) = s(R \circ f \circ R^t)$. □

If $f(r) = Mr + x$, choose $R \in \mathrm{SO}(3)$ such that $Rx = [s\ 0\ 0]^t$. Then

$$R \circ f \circ R^t(r) = RMR^t r + Rx \tag{25}$$

which, using the last lemma, has the same scope as f. Therefore, we will assume that f is of the form

$$f(r) = \begin{pmatrix} a & b & c \\ d & e & f \\ g & h & j \end{pmatrix} r + \begin{pmatrix} s \\ 0 \\ 0 \end{pmatrix}. \tag{26}$$

Lemma 12 *If $s(f) = [p]$ then $e = j$ and $h = -f$.*

Proof. Let $K = \{r \in \partial\mathbb{B} : r_1 = 0\}$. Then for $r \in K$, $\langle r, x\rangle = 0$ and

$$\langle r, fr\rangle = r^t Mr = er_2^2 + hr_2r_3 + fr_2r_3 + jr_3^2.$$

Also, since $\langle r, x\rangle = 0$, for every $r \in K$, $x_f(r)$ is binary symmetric. Note though, two binary symmetric channels have equal capacity if and only if they are equal, or if one is a reflection of the other about the diagonal of the unit square. Since the function that maps $r \mapsto x_f(r)$ is continuous, if $\{x_f(r) : r \in K\}$ was not a single point, it would have to be a line of binary symmetric channels, and thus f would not have constant capacity. Thus for $r \in K$, $\langle r, Mr\rangle$ must be constant. Choosing $r = e_2$ and $r = e_3$, we see that $e = j$. With this observation, we see that for a general $r \in K$,

$$e = r^t Mr = e + (h + f)r_2r_3,$$

implying that $h = -f$. □

We can now update the form of f to

$$f(r) = \begin{pmatrix} a & b & c \\ d & e & f \\ g & -f & e \end{pmatrix} r + \begin{pmatrix} s \\ 0 \\ 0 \end{pmatrix}. \tag{27}$$

From here out, we will continually assume that the scope of f is constant and that $s \neq 0$.

Lemma 13 *If $e = 0$, then M is skew-symmetric.*

Proof. If $e = 0$, then $c(x_f(e_2)) = 0$, and therefore $s(f) = [0]$. Noting that a classical channel has capacity 0 if and only if $P(0|0) = P(0|1)$, we see that $\langle r, Mr\rangle = 0$ for each $r \in \partial\mathbb{B}$. Using $r = e_1$, we see that $a = 0$. Additionally, using

$$r = \frac{1}{\sqrt{2}} \begin{pmatrix} 1 \\ 1 \\ 0 \end{pmatrix} \qquad \text{and} \qquad r = \frac{1}{\sqrt{2}} \begin{pmatrix} 1 \\ 0 \\ 1 \end{pmatrix}$$

we see that $b = -d$ and $c = -g$, respectively. □

We have shown that if $a = e = 0$ then M, must be skew-symmetric. To show that the off diagonal part of M must be skew-symmetric in general, we will be employing a result from Martin and Chatzikokolakis [24]. The computations are not elegant, but the idea is: in the unit square of channels, as one moves along lines of slope 1 toward the anti-diagonal, the capacity is non-increasing, and is strictly decreasing off the main diagonal; these lines of classical channels are those with constant determinant [24]. For a non-unital channel, when the off diagonal of M is not skew-symmetric, the classical channels that it generates are both symmetric and non-symmetric binary channels that have the same determinant. This immediately implies that the general binary channel, must have capacity strictly larger than the binary symmetric channel. Let $\{e_1, e_2, e_3\}$ be the standard basis for $\mathbb{R}^3$.

Proposition 14 *The off-diagonal of M must be skew-symmetric, and if $a = e$, then they both must be 0.*

Proof. Note that $\det(x_f(r)) = P(0|0) - P(0|1) = \langle r, Mr\rangle$ and that $\det\left(x_f(e_2)\right) = e$. For $r \in \partial\mathbb{B}$,

$$\langle r, Mr\rangle = r_1[(a - e)r_1 + (b + d)r_2 + (c + g)r_3] + e. \tag{28}$$

When $r = e_1$, $\langle r, Mr\rangle = a$. If $a = e$, then $\det(x_f(e_1)) = \det(x_f(e_2))$. However, $x_f(e_2)$ is binary symmetric and $x_f(e_1)$ is not. Therefore, from [24],

$$c(x_f(e_2)) \leq c(x_f(e_1)), \tag{29}$$

with equality if and only if both capacities are 0. Then for f to have constant scope, either a and e are both 0, or $a \neq e$. From Lemma 13, if $e = 0$, then M must be skew-symmetric.

In the event that $a \neq e$, take an $r \in \partial\mathbb{B}$ with $r_3 = 0$. Then for $e = \langle r, Mr\rangle$, from eqn. (28) $r_1 = -(b+d)/(a-e)r_2$. Since $r \in \partial\mathbb{B}$, $1 = r_1^2 + r_2^2$. Therefore,

$$r_2^2 = \left(1 + \frac{(b+d)^2}{(a-e)^2}\right)^{-1} \Rightarrow\ r_1 = \pm\frac{b+d}{a-e}\left(1 + \frac{(b+d)^2}{(a-e)^2}\right)^{-1/2}.$$

Then we have solved for $r \in \partial\mathbb{B}$ with $e = \langle r, Mr\rangle$. Unless $r = \pm e_2$, $x_f(r)$ is not binary symmetric, in which case $x_f(e_2) < x_f(r)$. Consequently, for f to have constant scope, then $b = -d$. By using an $r \in \partial\mathbb{B}$ with $r_2 = 0$, we can construct a similar argument that shows $c = -g$. □

We can now look toward the diagonal of the constant scope channel and further simplify its structure. Note that

$$g = \frac{1}{2}f + \frac{1}{2}s_z \circ f \circ s_z = \begin{pmatrix} a & 0 & 0 \\ 0 & e & f \\ 0 & -f & e \end{pmatrix} r + \begin{pmatrix} s \\ 0 \\ 0 \end{pmatrix} \tag{30}$$

Further we note that there exist rotations $P = 1 \oplus p$ and $Q = 1 \oplus q$, with $p, q \in M_2$, such that

$$(P \circ g \circ Q)r = \begin{pmatrix} a & 0 & 0 \\ 0 & e & -f \\ 0 & f & e \end{pmatrix} r + \begin{pmatrix} s \\ 0 \\ 0 \end{pmatrix}; \tag{31}$$

we know such P and Q exist, because the matrix

$$\begin{pmatrix} e & -f \\ f & e \end{pmatrix} \tag{32}$$

and its transpose have the same singular values and therefore, can be mapped to one another via multiplication on the left and right by rotations. We can then consider then channel

$$\frac{1}{2}g + \frac{1}{2}P \circ g \circ Q = \begin{pmatrix} a & 0 & 0 \\ 0 & e & 0 \\ 0 & 0 & e \end{pmatrix} r + \begin{pmatrix} s \\ 0 \\ 0 \end{pmatrix}, \tag{33}$$

which has the same capacity curve as f; then, without loss of generality, we can assume f takes the form of eqn. (33).

Proposition 15 *If the scope of f is constant, then $sgn(a) = sgn(e)$ and either $e = a = 0$, or $|e| > |a|$.*

Proof. Lets assume that $\mathrm{sgn}(a) \neq \mathrm{sgn}(e)$; then $\mathrm{sgn}(\langle e_1, Me_1\rangle) \neq \mathrm{sgn}(\langle e_2, Me_2\rangle)$. From the continuity of the inner product, there exists $r \in \partial\mathbb{B}$ with $0 = \langle r, Mr\rangle$. Then $x_f(r) = \frac{1}{2}(1+s, 1+s)$, which has 0 capacity. But when $e \neq 0$, $c(x_f(e_2)) \neq 0$, implying that for f to have constant scope, $\mathrm{sgn}(a) = \mathrm{sgn}(e)$.

From [23], we have the interlacing relation

$$M^- \leq f^- \leq M^+ \leq f^+,$$

where $M^\pm$ and $f^\pm$ are the largest and smallest capacities of the classical channels generated by M and f, respectively. If the scope of f is constant, then the last three inequalities turn into equalities. If $|e| \leq |a|$, then $M^- = 1 - H(e)$; note also though the $s(f) = [\mathrm{c}(x_f(e_2))] = [1 - H(e)]$, which implies that $M^+ = 1 - H(e)$. Consequently, $a = e$ which means both are 0 from a previous lemma. Thus, $|a| \leq |e|$, with equality only if both are 0. □

Corollary 16 *If $a = 0$ and f has constant scope, then $e = 0$ as well.*

Proof. If $a = 0$, then $\langle e_1, Me_1\rangle = 0$, and thus the induced classical channel is $1/2(1+s, 1+s)$; this channel has capacity 0. But also, the classical channel induced by $r = e_2$ is $1/2(1+e, 1-e)$, which only has capacity 0, if $e = 0$. □

We have now shown that if f has constant scope, then f can be *rotated* to

$$f(r) = \begin{pmatrix} a & b & c \\ -b & e & f \\ -c & -f & e \end{pmatrix} r + \begin{pmatrix} s \\ 0 \\ 0 \end{pmatrix}, \tag{34}$$

where $\mathrm{sgn}(a) = \mathrm{sgn}(e)$ and $|a| \leq |e|$, with equality if and only if both are 0. In this case, the classical channel generated by an $r \in \partial\mathbb{B}$ is

$$x_f(r) = \left(\frac{1 + (a-e)r_1^2 + e + sr_1}{2}, \frac{1 - (a-e)r_1^2 - e + sr_1}{2} \right), \tag{35}$$

and therefore, the curve of channels is described by a single variable. We can use these results to prove that the amplitude dampening channel does not have constant scope. Also, we can show that when f is rotated to the form of eqn. 34, given a fixed e and s, if there is an a that makes the scope constant, it must be unique. Additionally, using other inequalities we can further restrict the values of a, e and s. While this concludes captures most of the progress we have made on this problems, we do have the following conjecture:

Conjecture 17 *If a non-unital channel has constant scope, it's matrix part is skew-symmetric.*

To conclude the discussion on the non-unital capacity calculations and estimations, we have shown that if a channel has constant scope, then problem can be reduced from a 12 variable function to that of a single variable.

3.5 Quantum Sensing

The engineering challenges of building quantum enhanced technologies have proven great. The speed up over classical computation and the enhanced resolution of a quantum sensor, to name two, have not been fully realized due to the complexity of maintaining, manipulating, and measuring quantum states. However, in 2016, China reported an experimental implementation of a quantum radar that was able to detect stealth targets [25, 26]. While a staggering result, it is difficult to verify as the details were not made public. In [27], we provided a numerical model for the probability of detecting a test object using entangled states in the optical regime. This was not meant to foray into the debate over the usefulness or practicality of quantum illumination, but rather to provide a probability of detecting a circular test object based on the best commercially available technology and the standard theory of quantum illumination [28]. We assume access to the state-of-the-art commercialized technology for state generation and detection. We therefore considered the optical regime, but using such a short wavelength limits the range at which one can detect the presence of an object. Both the atmospheric attenuation and the relative roughness of most objects are range limiting factors in the optical regime. We considered objects of differing reflectivities and transmissivities, and then we plotted the probability of detection. First, we considered a 1.2 m in diameter circular object which scatters diffusely and has no specular component, sampling over 1s intervals. Fig. 4 plots the probability of detecting a test object of reflectivity 1/2 versus range; materials with similar reflectivity are ocean ice and matte aluminum [29]. We estimated that the probability of detecting this test object at 700m is a little over 80%. In fig. 5, we consider a less reflective object and plot the probability of detection when the reflectivity is $1/10$. From figs. 4 and 5, we estimated that at distances of 700 m and 400 m (respectively) the probability

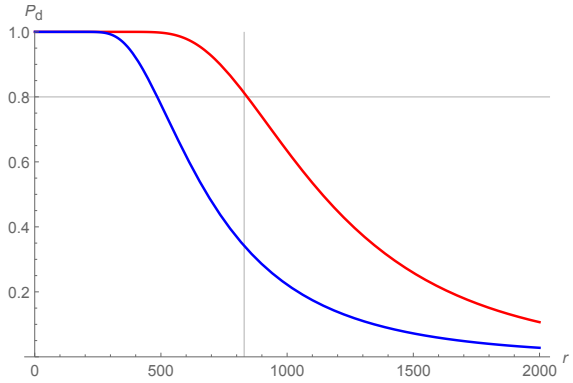

Fig. 4—Probability of detection plotted against the object's distance in meters for a diffuse object of reflectivity 1/2. The red line models optimal detection using entangled light, while the blue line models non-entangled light.

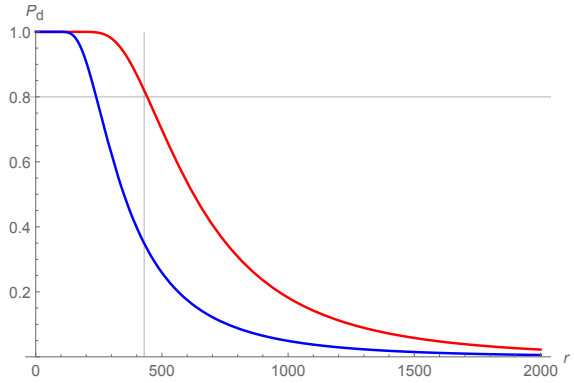

Fig. 5—Probability of detection plotted against the object's distance in meters for a diffuse object of reflectivity 1/10. The red line models optimal detection using entangled light, while the blue line models non-entangled light.

of detection is reduced by more than a factor of two when using non-entangled light versus entangled light; however, regardless of the improved detection probability, these ranges are extremely limiting. Note here, these figures only model the optimal detection method outlined in [28].

To show the extreme effect that diffuse scattering has on range, we modeled test objects that scattered specularly at optical wavelengths. For this, we assumed the test object is smaller than the diffuse object, having a diameter of 1 mm, sampling at 1 ms intervals. In fig. 6, we plotted the expected probability of detection when the reflectivity of the test object is 1/2. At a range of 8.2 km, we estimated that the probability

of decection is approximately 80% using an optimal receiver. Since the scattering is specular, we can even consider a test object with much lower reflectivity. In fig. 7, we plot the probability of detection for a specular object with a reflectivity of $1/10$; here, we estimate that we can detect the object with 80% efficiency at approximately 6.2 km using an optimal receiver. So even though the object is mostly transmissive, we estimated that we can still detect its presence with relativity high certainty at a range of kilometers. Comparing figs. 4 and 5 to figs. 6 and 7, the range for detecting a specular object significantly increases over that of an object that scatters diffusely. Note also, that in figs. 6 and 7 we considered the probability of detection with an optimal quantum receiver, which has yet to be realized, and a suboptimal quantum receiver based on the work done in [30]. In addition, for the specular objects we modeled, entangled light could increase the range by up to a factor of 1.25 over non-entangled light (for a detection probability of 80%).

From this work, we concluded that one of the most conspicuous challenges in significantly extending the detection range for optically diffuse object is to develop the corresponding technology for much longer wavelengths. If such technology existed, we expect that the range would dramatically increase for objects that appear 'rough' to an optical signal. However, this technology is in its infancy, and is not capable of producing the quantity of entangled pairs that one would need for an experiment that we modeled. In order to operate in the microwave wavelengths, for example, significant developments in generating and detecting microwave entangled states are needed. Additionally, we should note that there still seem to be massive engineering challenges to overcome before quantum illumination protocols could be deployed.

Additionally though, we reimagined this sensing protocol as a communication protocol. For this protocol, Alice would have a specular surface with low reflectivity and could use it in an application for low power covert communication. In such a scenario Alice would transfer information to Bob by obstructing photons sent from Bob in Alice's direction. Such a protocol would require very little power from Alice because she would not have to generate the signal that she is sending. Here, Alice sends information to Bob, but the information transfer would almost completely be powered by Bob: the presence of an object would allow Alice to send the classical bit 1 for example, and the absence would be a classical bit 0. In fig. 7, we estimate that even if Alice used an object of reflectivity $1/10$, the optimal bound predicts Bob could receive Alice's message at a distance of 6.2 km with 80% certainty, and at a distance of 5.8 km using the more conservative suboptimal estimate. Our model further estimates that if Alice used an object with reflectivity $1/100$, Bob could still receive her message with 80% efficiency at a range of 3.7 km (not plotted). Since most objects reflect diffusely, the system couldn't detect them at long distances. Therefore, any object that our system detected at these distances would likely be Alice's optical element. In addition, at this level, the contributions from the signal are indistinguishable from environmental noise. Combining that with the fact that Alice's object is small, and almost indistinguishable from a clear optical window, we opine that Alice could communicate with Bob in a covert nature. For full details of these results see [27, 31]

ACKNOWLEDGMENTS

The author is deeply indebted to Dr. Keye Martin who asked a battery of interesting questions that spawned the idea of this project. The author would also like to thank Dr. Daniel Bonior, Dr. Roderick Davidson, Dr. Marco Lanzagorta, and Dr. Keye Martin for their support, contributions, collaborations, discussions on philosophy, and artistic inspiration during the course of this project.

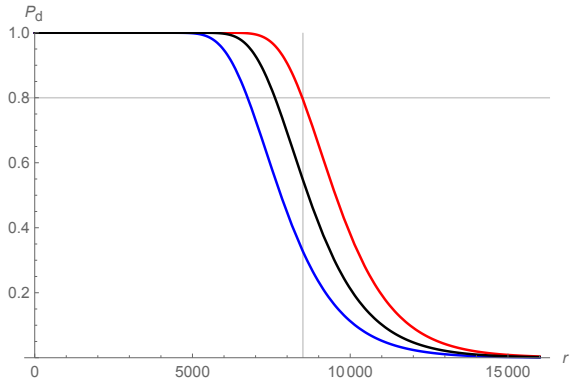

Fig. 6—Probability of detection plotted against the object's distance in meters for a specular object of reflectivity 1/2. The red line models detection using an optimal receiver and the black line models a suboptimal receiver, both using entangled light. The blue line models non-entangled light.

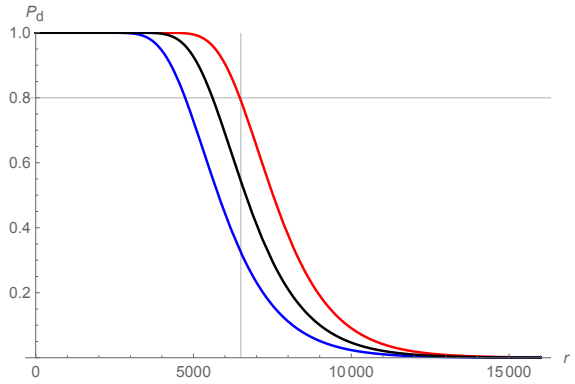

Fig. 7—Probability of detection plotted against the object's distance in meters for a specular object of reflectivity 1/10. The red line models detection using an optimal receiver and the black line models a suboptimal receiver, both using entangled light. The blue line models non-entangled light.

REFERENCES

1. T. Crowder and M. Lanzagorta, "The scope of a relativistic quantum process with spin-momentum entanglement," Proceedings of the International Conference on Unconventional Computation and Natural Computation (Springer), 2018, pp. 46–58.

2. T. Crowder and M. Lanzagorta, "Quantum information processing in the neighborhood of a black hole," *Nat. Comp.* **18**(3), 549–561 (2019).

3. M. Lanzagorta and T. Crowder, "Comment on "Wigner rotations and an apparent paradox in relativistic quantum information"," *Phys. Rev. A* **96**(2), 026101 (2017).

4. T. Cover and J. Thomas, *Elements of information theory* (John Wiley & Sons, 1999).

5. K. Martin, "The scope of a quantum channel," Proceedings of the Proceedings of Symposia in Applied Mathematics, volume 71, 2012, pp. 183–213.

6. M. Nielsen and I. Chuang, *Quantum Computation and Quantum Information* (Cambridge University Press, 2010).

7. K. Martin, "How to randomly flip a quantum bit," *Electronic Notes in Theoretical Computer Science* **270**(1), 81–97 (2011).

8. T. Crowder, *Representations of quantum channels*, PhD thesis (Howard University, 2013).

9. K. Martin, J. Feng, and T. Crowder, "Euclidean Representations of Quantum States," in *Horizons of the Mind. A Tribute to Prakash Panangaden*, pp. 454–457 (Springer, 2014).

10. T. Crowder, "A quantum representation for involution groups," *Electron. Notes in Theor. Comp. Sci.* **276**, 145–158 (2011).

11. L. Landau and R. Streater, "On Birkhoff's theorem for doubly stochastic completely positive maps of matrix algebras," *Linear algebra and its applications* **193**, 107–127 (1993).

12. D. Bonior and T. Crowder, "Noise Characterization of Two-Qubit Teleportation," *In Preperation* (2021).

13. T. Crowder and K. Martin, "Classical representations of qubit channels," *Electronic Notes in Theoretical Computer Science* **270**(2), 37–58 (2011).

14. T. Crowder and K. Martin, "Information theoretic representations of qubit channels," *Found. Phys.* **42**(7), 976–983 (2012).

15. M. Choi, "Completely positive linear maps on complex matrices," *Linear algebra and its applications* **10**(3), 285–290 (1975).

16. L. C. Céleri, V. Kiosses, and D. R. Terno, "Spin and localization of relativistic fermions and uncertainty relations," *Physical Review A* **94**(6), 062115 (2016).

17. P. L. Saldanha and V. Vedral, "Physical interpretation of the Wigner rotations and its implications for relativistic quantum information," *New Journal of Physics* **14**(2), 023041 (2012).

18. E. Taillebois and A. Avelar, "Spin-reduced density matrices for relativistic particles," *Physical Review A* **88**(6), 060302 (2013).

19. T. Choi, "Relativistic spin operator and Lorentz transformation of the spin state of a massive Dirac particle," *Journal of the Korean Physical Society* **62**(8), 1085–1092 (2013).

20. H. Bauke, S. Ahrens, C. H. Keitel, and R. Grobe, "Relativistic spin operators in various electromagnetic environments," *Physical Review A* **89**(5), 052101 (2014).

21. M. Lanzagorta, *Quantum information in gravitational fields* (Morgan & Claypool, 2014).

22. T. Crowder and M. Lanzagorta, "Gravitationally Invariant Subspaces in Quantum Computing," *Under Review* (2021).

23. K. Martin, T. Crowder, and J. Feng, "Quantum error reduction without coding," Proceedings of the Radar Sensor Technology XIX; and Active and Passive Signatures VI, volume 9461 (International Society for Optics and Photonics), 2015, p. 946114.

24. K. Chatzikokolakis and K. Martin, "A monotonicity principle for information theory," *Electronic Notes in Theoretical computer science* **218**, 111–129 (2008).

25. S. Chen, "The end of stealth? New Chinese radar capable of detecting 'invisible' targets 100km away," *South China Morning Post* (21 September 2016). URL `http://www.scmp.com/news/china/article/2021235/end-stealth-new-chinese-radar-capable-detecting-invisible-targets-100km`.

26. E. Kania and S. Armitage, "Disruption under the radar: Chinese advances in quantum sensing," *China Brief* **17**(11) (2017). URL `https://jamestown.org/program/disruption-under-the-radar-chinese-advances-in-quantum-sensing/.`

27. T. Crowder and M. Lanzagorta, "Detection and communication with entanglement," Proceedings of the 2018 IEEE Conference on Antenna Measurements & Applications (CAMA) (IEEE), 2018, pp. 1–4.

28. S. H. Tan, B. I. Erkmen, V. Giovannetti, S. Guha, S. Lloyd, L. Maccone, S. Pirandola, and J. H. Shapiro, "Quantum illumination with Gaussian states," *Physical review letters* **101**(25), 253601 (2008).

29. M. Bass, E. W. Van Stryland, D. R. Williams, and W. L. Wolfe, *Handbook of optics*, volume 2 (McGraw-Hill New York, 1995).

30. S. Guha and B. I. Erkmen, "Gaussian-state quantum-illumination receivers for target detection," *Physical Review A* **80**(5), 052310 (2009).

31. T. Crowder and M. Lanzagorta, "Low brightness, entanglement-based, semi-passive private communication protocol," Feb 2021. US Patent 10,924,191.